


Article

Pseudomonas aeruginosa *mexR* and *mexEF* Antibiotic Efflux Pump Variants Exhibit Increased Virulence

Mylene Vaillancourt ¹, Sam P. Limsuwanarot ¹, Catherine Bresee ², Rahgavi Poopalarajah ³ and Peter Jorth ^{1,4,5,*} 

¹ Department of Pathology and Laboratory Medicine, Cedars-Sinai Medical Center, Los Angeles, CA 90048, USA; Mylene.Vaillancourt@cshs.org (M.V.); Podsawee.Limsuwanarot@cshs.org (S.P.L.)

² Biostatistics Core, Cedars-Sinai Medical Center, Los Angeles, CA 90048, USA; Catherine.Bresee@cshs.org

³ Department of Biological Sciences, University of Calgary, Calgary, AB T2N 1N4, Canada; Rahgavi.Poopalarajah@ucalgary.ca

⁴ Department of Medicine, Cedars-Sinai Medical Center, Los Angeles, CA 90048, USA

⁵ Department of Biomedical Sciences, Cedars-Sinai Medical Center, Los Angeles, CA 90048, USA

* Correspondence: Peter.Jorth@cshs.org; Tel.: +1-310-967-2712

Abstract: Antibiotic-resistant *Pseudomonas aeruginosa* infections are the primary cause of mortality in people with cystic fibrosis (CF). Yet, it has only recently become appreciated that resistance mutations can also increase *P. aeruginosa* virulence, even in the absence of antibiotics. Moreover, the mechanisms by which resistance mutations increase virulence are poorly understood. In this study we tested the hypothesis that mutations affecting efflux pumps can directly increase *P. aeruginosa* virulence. Using genetics, physiological assays, and model infections, we show that efflux pump mutations can increase virulence. Mutations of the *mexEF* efflux pump system increased swarming, rhamnolipid production, and lethality in a mouse infection model, while mutations in *mexR* that increased expression of the *mexAB-oprM* efflux system increased virulence during an acute murine lung infection without affecting swarming or rhamnolipid gene expression. Finally, we show that an efflux pump inhibitor, which represents a proposed novel treatment approach for *P. aeruginosa*, increased rhamnolipid gene expression in a dose-dependent manner. This finding is important because rhamnolipids are key virulence factors involved in dissemination through epithelial barriers and cause neutrophil necrosis. Together, these data show how current and proposed future anti-Pseudomonas treatments may unintentionally make infections worse by increasing virulence. Therefore, treatments that target efflux should be pursued with caution.

Keywords: *Pseudomonas*; efflux pumps; virulence; evolution; antibiotic resistance; cystic fibrosis



Citation: Vaillancourt, M.; Limsuwanarot, S.P.; Bresee, C.; Poopalarajah, R.; Jorth, P. *Pseudomonas aeruginosa* *mexR* and *mexEF* Antibiotic Efflux Pump Variants Exhibit Increased Virulence. *Antibiotics* **2021**, *10*, 1164. <https://doi.org/10.3390/antibiotics10101164>

Academic Editor: Paul M. Beringer

Received: 31 August 2021

Accepted: 24 September 2021

Published: 25 September 2021

Publisher's Note: MDPI stays neutral with regard to jurisdictional claims in published maps and institutional affiliations.



Copyright: © 2021 by the authors. Licensee MDPI, Basel, Switzerland. This article is an open access article distributed under the terms and conditions of the Creative Commons Attribution (CC BY) license (<https://creativecommons.org/licenses/by/4.0/>).

1. Introduction

Pseudomonas aeruginosa is a ubiquitous Gram-negative bacterium that colonizes a wide range of environments [1]. This environmental flexibility is due to its high adaptability to changing conditions and is driven by substantial metabolic versatility, expression of a large array of virulence factors, and extensive adaptive transport and efflux systems [2]. *P. aeruginosa* is infamous for causing serious nosocomial infections, such as burn wound infections and ventilator-associated pneumonia [3], and it is the predominant pathogen causing chronic infections in cystic fibrosis (CF) [4].

During chronic infections, *P. aeruginosa* adapts to the CF lung environment by decreasing production of virulence factors and evolves to become antibiotic resistant [5–7]. Even more complicated, populations of *P. aeruginosa* within patients evolve high degrees of diversity and within-patient variability, where contemporary sibling cells that have descended from a common ancestor can differ in antibiotic susceptibilities and virulence factor production [8–11]. *P. aeruginosa* virulence mechanisms include attachment to cells (e.g., pili), induction of host damage (e.g., DNase, proteases), competition with the host

for nutrients, and the secretion of surfactant molecules such as rhamnolipids which cause neutrophil necrosis and permit dissemination [12–14]. Virulence factors usually trigger an exacerbated inflammatory response by the innate immune system, with macrophages and neutrophils as the first line of defense [15]. Thus, it has been proposed that decreasing virulence factor production attenuates the host inflammatory response and favors bacterial colonization of the lung during CF chronic infections.

In addition to the host pressures that affect virulence, bacteria colonizing CF lungs also experience intense antibiotic pressure due to mono and combination therapies including aminoglycosides, quinolones, and β -lactams [16]. This environment strongly favors the selection of antibiotic-resistant strains. Some of the best characterized antibiotic resistance features are efflux pump systems that expel antibiotics out of the cell. For example, we previously showed that *nalD* and *mexR* genes, both encoding for transcriptional repressors of the MexAB-OprM efflux pump [17–19], were recurrently mutated under aztreonam selection [20]. *P. aeruginosa* with mutations in *nalD* and *mexR* overexpress the MexAB-OprM efflux pump, rendering them multidrug resistant [17,19,21]. Moreover, mutations in these two genes have been found in anywhere from 7–47% of clinical isolates in various studies [20–24]. Importantly, strains with mutations in *nalD* and *mexR* evolved under aztreonam selection showed increased virulence *in vivo*, challenging the longstanding theory that antibiotic-resistance mutations inherently pay fitness costs that attenuate virulence [20]. However, whether these mutations increase virulence in an efflux-dependent manner remains unknown.

In this study, we sought to investigate the mechanisms involved in the hypervirulence of a mutant *P. aeruginosa* strain, PAO1-AzEvB8, that was experimentally evolved in a previous study during cyclic aztreonam exposure [20]. Because this strain was previously shown to have a mutation in *mexR*, we hypothesized that its hypervirulence could be attributed to the increased expression of the MexAB-OprM efflux pump. We explore this hypothesis using a combination of genome sequencing, genetics, transcriptional reporter assays, and infection models.

2. Results

2.1. Deletion of *mexAB* Restores Aztreonam Susceptibility of Evolved *P. aeruginosa*

Previously, we used experimental evolution with cyclical exposure to aztreonam to evolve the aztreonam resistant strain PAO1-AzEvB8 [20]. Strain PAO1-AzEvB8 was found to have a nonsense mutation in *mexR* (E118*) and complementation with a wild-type (WT) *mexR* gene restored aztreonam susceptibility [20]. Because *mexR* mutations have been shown to increase expression of the *mexAB-oprM* efflux pump operon [19,21], which encodes the pump that effluxes aztreonam, we hypothesized that deletion of *mexAB* in PAO1-AzEvB8 would restore aztreonam susceptibility. We generated clean *mexAB* deletions in both WT PAO1 and in PAO1-AzEvB8, and the PAO1-AzEvB8 Δ *mexAB* strain was equally susceptible to aztreonam by a gradient diffusion assay as the PAO1 Δ *mexAB* strain (Figure 1A); the mode minimum inhibitory concentrations (MIC) for Δ *mexAB* strains was 0.19 μ g/mL, compared to 16 μ g/mL for PAO1-AzEvB8 and 1.0 μ g/mL for WT PAO1. This showed that *mexAB* was required for aztreonam resistance of the of the PAO1-AzEvB8 mutant.

2.2. Deletion of *mexAB* Does Not Affect Virulence of Evolved *P. aeruginosa*

In addition to exhibiting increased aztreonam resistance relative to WT PAO1, strain PAO1-AzEvB8 also displayed increased killing of mice in an acute murine infection model. We hypothesized that, similar to the aztreonam resistance, the increased virulence of PAO1-AzEvB8 would be dependent upon *mexAB* which was overexpressed in this strain. Surprisingly, the PAO1-AzEvB8 Δ *mexAB* strain was equally virulent to strain PAO1-AzEvB8 (Figure 1B), indicating that the increased virulence was not dependent on *mexAB* alone. This was even more unexpected since PAO1 Δ *mexAB* was less virulent than WT PAO1

(Figure 1B). This suggested that another gene or mutation was involved in the enhanced virulence of PAO1-AzEvB8.

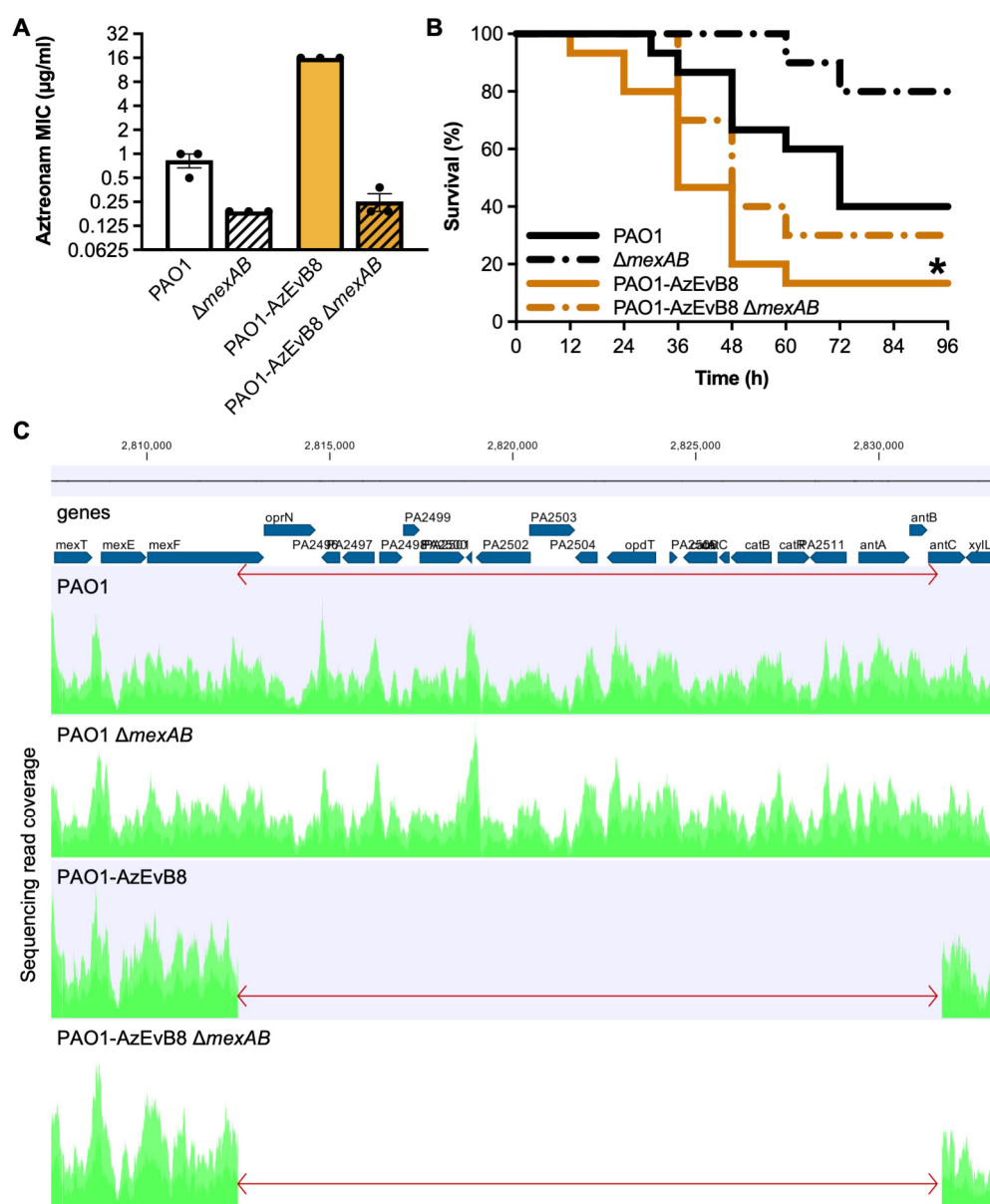


Figure 1. MexAB-OprM is not involved in the PAO1-AzEvB8 mutant in vivo virulence. (A) Deletion of the *mexAB* genes abrogates aztreonam resistance in strain PAO1-AzEvB8. Aztreonam MICs were determined by gradient diffusion assays ($n = 3$ replicates/group; MIC: minimum inhibitory concentration). (B) *mexAB* deletion in PAO1-AzEvB8 mutant does not significantly improve mouse survival following acute lung infection. Log-rank test was used to compare survival curves. * $p < 0.05$ compared to WT PAO1; $n = 10$ –15 mice/group. (C) Genome diagram showing coverage of sequencing reads aligning to the region spanning *mexEF* through *xylZ*. The 19,233 bp deleted region (indicated by the red arrow) in strains PAO1-AzEvB8 and PAO1-AzEvB8 $\Delta mexAB$ begins at the 3' end of *mexF* and continues through the 5' region of *antC*. Genome coverage plots generated from sequencing read alignments to the PAO1 reference genome are indicated in green.

2.3. Genome Sequencing Reveals a Previously Undetected 19 kb Deletion in PAO1-AzEvB8

To determine whether another mutation may be present in the strain PAO1-AzEvB8, we performed whole genome sequencing on strains PAO1 (WT parent strain), PAO1 $\Delta mexAB$, PAO1-AzEvB8, and PAO1-AzEvB8 $\Delta mexAB$. Using this approach, we found that

relative to WT PAO1, a large ~19 kb deletion affecting 21 genes spanning *mexF* through *antC* was present in the PAO1-AzEvB8 and PAO1-AzEvB8 $\Delta mexAB$ strains (Figure 1C). This deletion was not detected by the genome sequencing in our original study despite >10-fold sequencing coverage of the genome [20]. The genes affected by this mutation included *mexF* and *oprN* which form part of the *mexEF-oprN* efflux pump operon. Previously, these genes have been linked to the swarming phenotype in *P. aeruginosa*, with studies indicating that strains overexpressing *mexE* have decreased swarming [25,26]. This led us to predict that the *mexF* mutation could lead to increased swarming and rhamnolipid production in the PAO1-AzEvB8 strain.

2.4. Mutation of *mexEF* Increases Swarming While *mexR* Mutation Does not

Based on the deletion of a large part of the *mexEF-oprN* operon in strain PAO1-AzEvB8, we hypothesized that this strain would exhibit increased swarming, as would mutants lacking *mexEF*. To test this, we generated a strain with the *mexEF* genes deleted in a WT PAO1 background. Gradient diffusion susceptibility testing showed that the PAO1 $\Delta mexEF$ strain was more susceptible to both ciprofloxacin and chloramphenicol than WT PAO1 (mode ciprofloxacin MICs: PAO1 $\Delta mexEF$ 0.125 $\mu\text{g/mL}$ vs. WT PAO1 0.5 $\mu\text{g/mL}$; mode chloramphenicol MICs: PAO1 $\Delta mexEF$ 48 $\mu\text{g/mL}$ vs. WT PAO1 >256 $\mu\text{g/mL}$; $n = 3$). Swarming assays were performed using the WT PAO1, PAO1-AzEvB8, PAO1 $\Delta mexEF$, and PAO1 $\Delta mexR$ strains. As predicted, the PAO1-AzEvB8 strain displayed more swarming than WT, as did PAO1 $\Delta mexEF$ (Figure 2A,B). In contrast, deletion of *mexR* in a WT PAO1 background did not affect swarming (Figure 2A,B). Next, we tested whether *mexEF* mutations led to increased rhamnolipid production, because rhamnolipids are involved in swarming and cause necrosis of neutrophils [13]. A *rhlA-gfp* transcriptional reporter was transformed into strains PAO1, PAO1 $\Delta mexEF$, PAO1 $\Delta mexAB$, PAO1 $\Delta mexR$, and PAO1-AzEvB8 and *rhlA* expression was monitored during the course of growth. Consistent with the swarming phenotypes, PAO1 $\Delta mexEF$ had the highest *rhlA* expression (Figure 2C). However, unexpectedly, PAO1-AzEvB8 had less *rhlA* expression than PAO1 $\Delta mexEF$, similar *rhlA* expression to WT PAO1, and slightly more *rhlA* expression than PAO1 $\Delta mexAB$ and PAO1 $\Delta mexR$ strains (Figure 2C). Together these data showed that the PAO1-AzEvB8 strain had a hyper-swarming phenotype, a *mexEF* deletion mutation was sufficient to increase swarming, and a *mexR* deletion mutation alone does not affect swarming.

To further study the effects of *mexEF* mutations on swarming and rhamnolipid gene expression, we also investigated these phenotypes using transposon (Tn) mutants. Swarming assays showed the PAO1 Tn mutants in *mexE*, *mexF*, and *oprN* all exhibited increased swarming relative to a Tn mutant control (PA3033), which has been shown to be a neutral Tn mutation for numerous phenotypes. As above, a *mexR* Tn mutant showed the same levels of swarming as the Tn mutant control.

2.5. Deletion of either *mexR* or *mexEF* Increases *P. aeruginosa* Virulence

To better understand the increased virulence of the PAO1-AzEvB8 strain, we analyzed the virulence of PAO1 $\Delta mexR$ and PAO1 $\Delta mexEF$ strains to determine if either the *mexR* or *mexF* mutations detected in the PAO1-AzEvB8 strain could have contributed to the increased virulence. Using an acute murine lung infection model, we found that both PAO1 $\Delta mexR$ and PAO1 $\Delta mexEF$ killed the infected mice significantly faster than the WT PAO1 strain (Figure 3). These findings suggest that either of the two mutations present in the PAO1-AzEvB8 were sufficient to increase the virulence, relative to the WT parent strain.

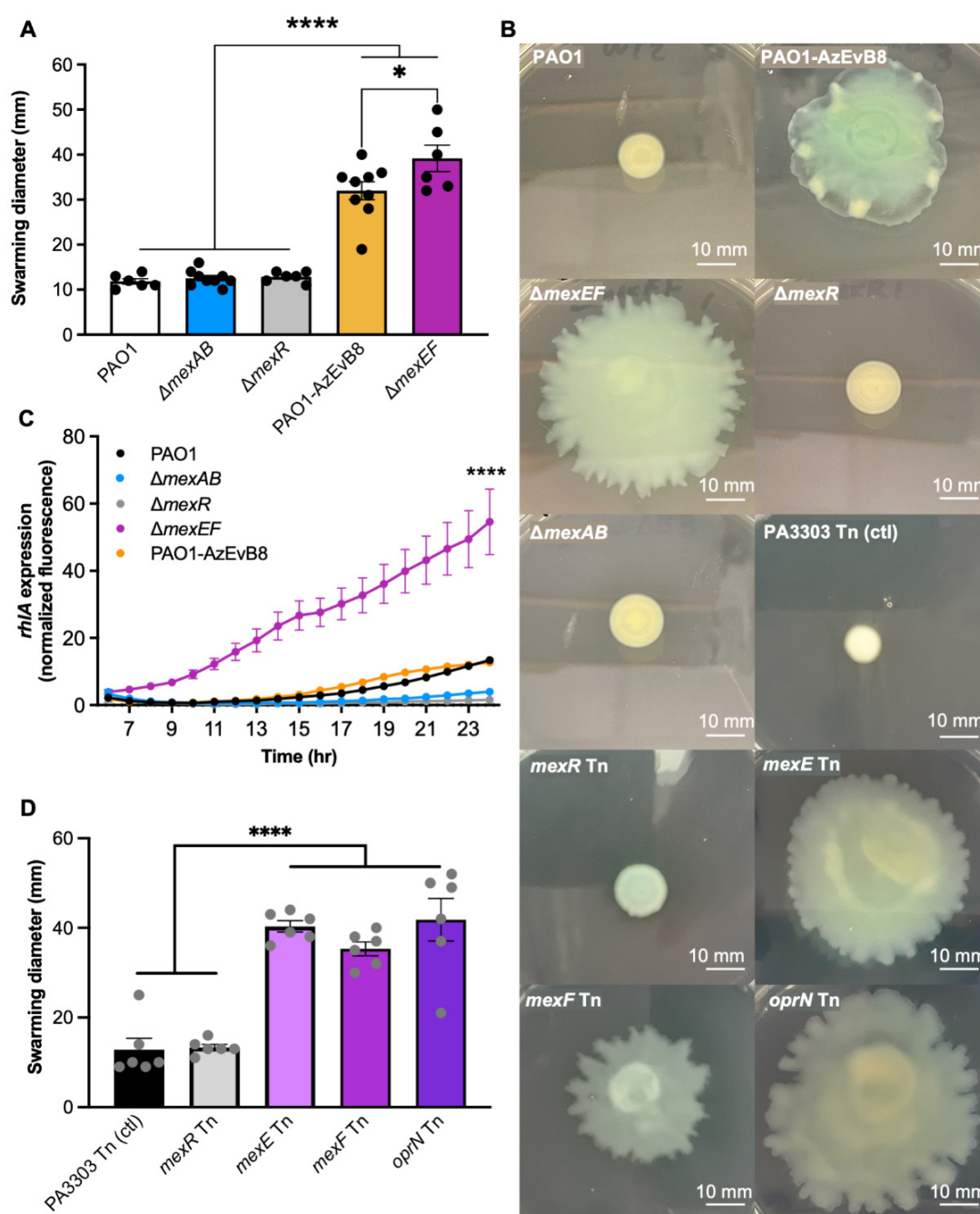


Figure 2. MexEF-OprN mutation increases swarming motility and biosurfactant production. **(A)** Swarming is increased in the PAO1-AzEvB8 and $\Delta mexEF$ strains. Measurement of the swarming motility in different *mexAB-oprM* and *mexEF-oprN* mutants after 24 h, $n = 6-7$ replicates/group. **(B)** Representative images of swarming motility from panels (A,D). Scale bars indicate 10 mm. **(C)** Rhamnolipid gene expression is increased in the $\Delta mexEF$ strain. Rhamnolipid production measured by quantification of *rhlA* gene expression using a *rhlA-gfp* promoter reporter fusion to measure GFP fluorescence over time. Gene expression was calculated as area under the curve for each strain and compared to all other groups, $n = 6-7$ replicates/group. **(D)** Swarming is increased in *mexE*, *mexF*, and *oprN* PAO1 transposon mutant strains. Measurement of the swarming motility in different *mexR* and *mexEF-oprN* transposon mutants vs. a neutral Tn mutant control (PA3303) after 24 h, $n = 5-12$ replicates/group. For all panels, * $p < 0.05$, **** $p < 0.0001$, one-way ANOVA, followed by a Tukey's multiple comparisons test.

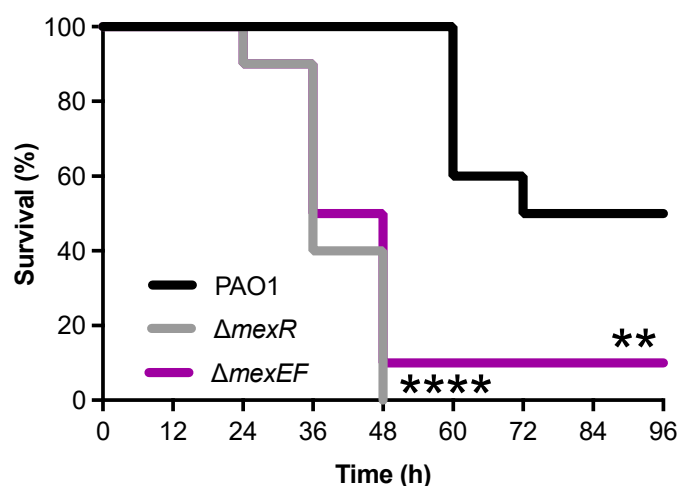


Figure 3. MexAB-OprM overexpression and MexEF-OprN deletion exhibit increased in vivo virulence. Both $\Delta mexR$ and $\Delta mexEF$ mutations in WT PAO1 significantly reduce mouse survival during an acute lung infection compared to WT PAO1 (WT). Survival times were tested across strata with a Bonferroni-adjusted log-rank test: ** $p < 0.005$ and **** $p < 0.0001$ compared to WT PAO1, $n = 10$ mice/group.

2.6. Efflux Pump Inhibition Increases Rhamnolipid Virulence Factor Expression

The swarming assays and mouse virulence experiment suggested that loss of the *mexEF* efflux pump was sufficient to increase swarming, rhamnolipid expression, and virulence in a mouse lung infection model. Therefore, we hypothesized that inhibition of efflux pump activity would lead to increased rhamnolipid gene expression. To test this, we exposed the PAO1 *attB::rhlA-gfp* reporter strain to increasing concentrations of the PA β N efflux pump inhibitor [27]. As hypothesized, increasing concentrations of PA β N from 0–25 $\mu\text{g/mL}$ led to increased *rhlA* rhamnolipid gene expression in a dose-dependent manner (Figure 4A). This showed that a broad-spectrum efflux pump inhibitor could increase the expression of an important virulence factor.

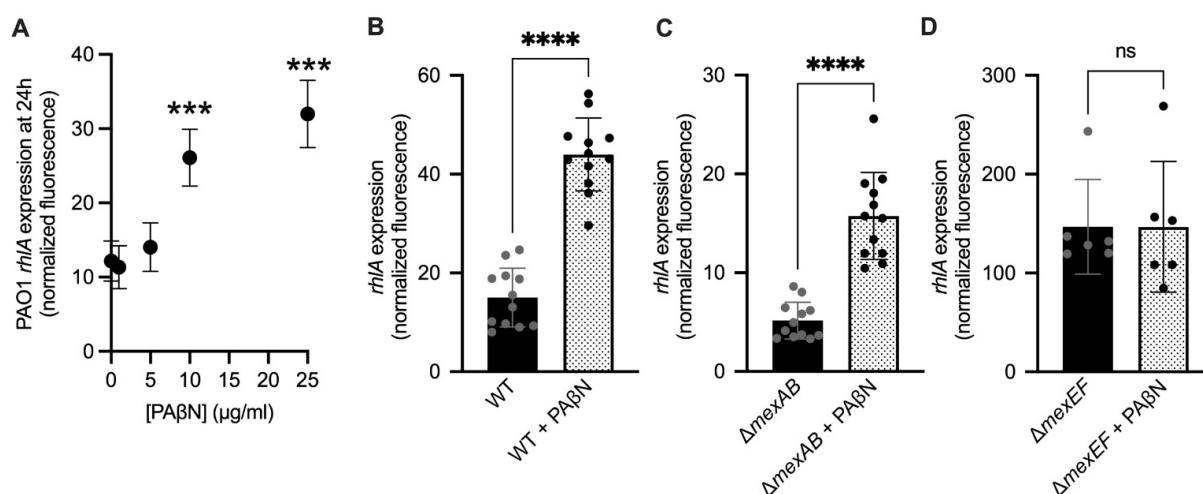


Figure 4. Rhamnolipid gene expression is induced by the Pa β N efflux pump inhibitor. (A) *rhIA* expression in WT PAO1 *attB::rhlA-gfp* treated with 0–25 $\mu\text{g/mL}$ PA β N as measured by GFP fluorescence from the *attB::rhlA-gfp* promoter reporter fusion at 24 h (** $p < 0.0005$, compared 0, 1, and 5 $\mu\text{g/mL}$, one-way Brown–Forsythe and Welch ANOVA followed by Dunnett’s T3 multiple comparisons test, $n = 6$ replicates/group). (B–D) *rhIA* expression in PAO1 *attB::rhlA-gfp* (B), PAO1 $\Delta mexAB$ *attB::rhlA-gfp* (C), and PAO1 $\Delta mexEF$ *attB::rhlA-gfp* (D), treated with or without 25 $\mu\text{g/mL}$ PA β N as measured by GFP fluorescence from the *attB::rhlA-gfp* promoter reporter fusion at 24 h. Gene expression was calculated as GFP fluorescence normalized to cell density (**** $p < 0.0001$; ns: not significant, $p > 0.05$, one-way Brown–Forsythe and Welch ANOVA followed by Dunnett’s T3 multiple comparisons test, $n = 6$ –12 replicates/group).

Because PA β N can inhibit both MexEF-OprN and MexAB-OprM, we tested the hypothesis that the PA β N inhibitor was increasing rhamnolipid gene expression in a *mexEF*-dependent manner. We incubated WT PAO1, PAO1 Δ *mexAB*, and PAO1 Δ *mexEF* *rhlA*-gfp reporter strains with or without 25 μ g/mL PA β N for 24 h. As predicted, PA β N increased *rhlA* gene expression in WT PAO1 and PAO1 Δ *mexAB* strains relative to untreated controls (Figure 4A–C), but not in the PAO1 Δ *mexEF* strain (Figure 4D). This shows that the increase of *rhlA* expression is occurring via inhibition of MexEF-OprN, not MexAB-OprM.

3. Discussion

3.1. Deletion of *mexEF* and Overexpression of *mexAB* through *mexR* Mutation Can Each Increase Virulence of *P. aeruginosa*

Here we showed that two different mutations affecting efflux pumps that evolved in response to aztreonam selective pressure can increase *P. aeruginosa* virulence in the absence of antibiotic treatment. These findings are interesting because one mutation, *mexR*, leads to overexpression of the MexAB-OprM efflux pump, while the other mutation conferred the loss-of-function of a second efflux pump, *mexEF-oprN*. We also showed that deletion of *mexEF* caused increased swarming, likely due to increased *rhlA* gene expression, which was demonstrated using a rhamnolipid gene expression reporter. Finally, we showed that MexEF-OprN efflux pump inhibition can have the unexpected effect of increasing rhamnolipid gene expression. This observation is important because rhamnolipids can cause necrosis of neutrophils and are also involved in the penetration of *P. aeruginosa* through epithelial barriers [13,14]. Altogether, these data highlight how antibiotic selection can unexpectedly increase virulence through multiple pathways.

3.2. Understanding Why *rhlA* Was Not Expressed in the PAO1-AzEvB8 Strain That Exhibited Greater Swarming Than WT

One curious result was that the PAO1-AzEvB8 strain did not overexpress *rhlA* relative to WT PAO1, despite exhibiting increased swarming. Because this strain had a large deletion mutation that included the 3' end of *mexF*, we expected it to exhibit elevated *rhlA* expression similar to the PAO1 Δ *mexEF* strain. One possible explanation is that with an intact *mexE* gene, the increase in *rhlA* relative to WT may be less pronounced than when both *mexE* and *mexF* are deleted. This is somewhat apparent in the quantification of the swarming assays where the swarming zone of PAO1 Δ *mexEF* was slightly larger than PAO1-AzEvB8. Another possible explanation is that the swarming assays were performed using semi-solid 0.5% agar plates, whereas the *rhlA* expression assays were done in broth cultures. In future work we plan to explore whether differences in *rhlA* expression are detectable during infection, which is where it is likely most relevant.

3.3. Relationship of These Findings to Previous Research

Overall, these results are consistent with previous studies which found that *P. aeruginosa* *nfxC* mutants, which overexpress *mexEF-oprN*, do not swarm and exhibit decreased *rhlA* expression relative to WT [26]. Likewise, these data also align with a study by Cosson et al. which found that *P. aeruginosa* *nfxC* mutants were avirulent in a rat acute pneumonia infection model, and virulence could be partially restored in the *nfxC* mutant by deleting *mexE* [28]. An important distinction is that, to our knowledge, it had not previously been shown that deletion of *mexEF* in a WT genetic background can increase virulence.

3.4. Differences among Infection Models Help Explain Why Previous Studies Concluded Different Effects of Efflux Pump Inhibition on Virulence

While our data agree with the studies discussed above, the finding that the Δ *mexEF* strain was more virulent than WT in the acute murine lung infection does appear to conflict other previous research related to efflux pump inhibition. In a study from Hirakata et al., PA β N was shown to reduce the intracellular invasion of Madin–Darby canine kidney epithelial cell monolayers by *P. aeruginosa* [29], which appears inconsistent with our findings. One simple explanation for this difference is that we were not measuring

intracellular invasion in our model. Instead, we measured virulence by survival following acute pneumonia, which we argue is more similar to human lung infections because neutrophils and epithelial barriers are present that can be harmed by the excess rhamnolipid produced in *mexEF* mutants and bacteria treated with PA β N. In another study, PA β N reduced the swarming and killing of *Galleria mellonella* larvae [30]. Again, slight differences in the infection model and the swarming assay could help explain differences from the present study. For example, the medium used for the swarming assay is different from the present study [30]. The *G. mellonella* infection model is also quite distinct from the mouse infection model used here, as it seems to be primarily affected by type III secretion [31] and lipopolysaccharide [32], and the role of rhamnolipids in the *G. mellonella* model is less clear. Therefore, we believe that differences in experimental design can account for the differences in interpretation of the effects of the PA β N efflux pump inhibitor. Future experiments will be required to determine whether PA β N and similar efflux pump inhibitors enhance or decrease virulence in mammalian infections.

3.5. Relevance of *mexEF* Mutations in *P. aeruginosa* Clinical Isolates

While *mexR* mutations have been identified in countless *P. aeruginosa* clinical isolates in previous studies [24,33], mutations directly affecting *mexEF* have not been as commonly described. Previous work has shown that mutations in *mexT*, the transcriptional activator of *mexEF*, are very common and these mutants were dubbed *nfxC*-type mutants for their resistance to norfloxacin [34,35]. Additionally, several studies have also examined *mexE* gene expression in large sets of clinical isolates, and in some strains *mexE* expression was reported to be less than WT, or completely undetected [22,36,37]. This suggests that these strains have either lost function of *mexT* or may potentially have deletions in *mexE*. This raises the possibility that these clinical isolates would also exhibit increased swarming, increased rhamnolipid production, and be more virulent than other clinical isolates, though this has not yet been investigated. We plan to test these phenotypes in clinical isolates with reduced *mexE* expression in the future.

3.6. Implications for CF and the Use of Efflux Pump Inhibitor as Potential Therapies

These results have several implications that are particularly relevant to CF treatment, including currently used anti-Pseudomonal therapies, as well as proposed new therapies.

First, these data show how aztreonam, a common antibiotic used to treat *P. aeruginosa* infections in people with CF, can select for not one, but two different mutations that increase *P. aeruginosa* virulence. This may help explain why a recent clinical observational study found that people with CF that were infected with aztreonam-resistant *P. aeruginosa* were more likely to experience pulmonary exacerbations and be hospitalized than people infected with aztreonam-susceptible *P. aeruginosa* [38]. If the isolates in those patients evolved mutations in either *mexR* or *mexEF-oprN*, then this could lead to increased virulence and lung damage in these individuals. Future work investigating the prevalence and association of these mutations with clinical outcomes will help test this theory.

Second, these data show that efflux pump inhibitors might have unexpected negative consequences on infections in people. Efflux pump inhibitors such as PA β N can inhibit efflux and potentiate other antibiotics that would normally be expelled through those pumps [27]. However, the experiments presented here show that inhibiting or deleting one efflux pump, MexEF-OprN, can have the unintended consequence of increasing rhamnolipid gene expression. Thus, inhibitors that affect MexEF-OprN may not be good candidates for use clinically. Instead, it would be more beneficial to identify more specific efflux pump inhibitors. For example, the MexAB-OprM-specific efflux pump inhibitor D13-9001 [39] could be used to block MexAB-OprM without inhibiting MexEF-OprN, and this could make *P. aeruginosa* more susceptible to other antibiotics and reduce virulence, since *mexAB* deletion mutants are less virulent than WT *P. aeruginosa*, as shown here and in other research [40]. Our data highlight the need to explore these types of precise approaches in future research using animal infection models.

3.7. Limitations of the Present Work

It is also important to acknowledge the limitations of this work. First, the strain PAO1-AzEvB8 that was the focus of the present study was not an actual clinical isolate and it is unclear how frequently mutants arise that have both *mexR* and *mexEF* mutations. As mentioned above, literature suggests that *mexR* mutations are very common in CF, and that clinical isolates can display varying degrees of *mexE* gene expression [20,22,24,33,36,37], so we feel that this study still has relevance to real-world *P. aeruginosa* infections.

The second primary limitation to this work is that the mouse model analyzed does not perfectly model the chronic infections that affect people with CF. One weakness is that this model does not capture the types of nutrient and biochemical properties present in CF that can affect *P. aeruginosa* antibiotic tolerance and virulence factor expression [41–44]. However, one strength to this model is that it does recapitulate the airway epithelial cell barrier and neutrophils present in CF infections that are susceptible to rhamnolipid-mediated toxicity [13,14]. To explore the effects of these mutations on other aspects of CF lung disease, future work could utilize chronic infection models in rodents or the more recently developed CF ferret and pig models [14,45–48].

One final limitation to this work is that the deletion mutants have not been complemented. Therefore, it is possible that the swarming and virulence phenotypes could be driven by the off-target effects of the generated mutations. We believe this is unlikely because we were able to reproduce identical phenotypes in multiple strains possessing related mutations. For example, the PAO1-AzEvB8 strain has both a *mexR* null mutation and *mexEF* deletion mutation, yet we only saw the swarming phenotype increased in the PAO1-AzEvB8 and Δ *mexEF* strains, not the Δ *mexR* or Δ *mexAB* strains. This suggests that the swarming phenotype in the PAO1-AzEvB8 strain is driven by its *mexEF* mutation. This was also supported by experiments with Tn mutants, where we observed increased swarming in *mexE*, *mexF*, and *oprN* Tn mutants, but not in a *mexR* Tn mutant. An additional caveat is that the clean deletion mutation in the PAO1 Δ *mexEF* strain was not generated in-frame with the *mexE* and *mexF* coding sequences, whereas the *mexR* and *mexAB* deletion constructs were generated in-frame with the original genes. Therefore, it is possible that a small peptide may be transcribed in the Δ *mexEF* strain that is out-of-frame (+1) relative to the *mexEF-oprN* coding sequences. This could have two consequences independent of the *mexEF* deletion. First, the Δ *mexEF* strain phenotypes could be caused by this novel peptide and not the *mexEF* deletion which was confirmed by whole genome sequencing. We think this is unlikely because the other phenotypes of this strain, including increased antibiotic susceptibilities to ciprofloxacin and chloramphenicol are consistent with previous studies of *mexE* mutants [26,35]. The other possibility is that these phenotypes could be caused by the effects of the *mexEF* deletion that prevent normal expression of *oprN*. Even if this were true, the phenotypes would still be consistent with the overall loss-of-function of the *mexEF-oprN* efflux pump, which is consistent with our conclusions. Long-term, we plan to perform complementation studies to tease out whether the swarming, rhamnolipid, and virulence phenotypes are due to loss-of-function of all three genes in the *mexEF-oprN* operon, or if phenotypes can be caused by mutation by each of the individual genes.

4. Materials and Methods

4.1. Bacterial Strains and Growth Conditions

Bacterial strains and plasmids are listed in Table S1. Mutant strains were derived from WT PAO1, which was obtained from Colin Manoil's laboratory at the University of Washington [49]. Tn mutants were also obtained from Colin Manoil's laboratory at the University of Washington and they were grown from freezer stock on Luria–Bertani (LB) agar with 10 µg/mL tetracycline [49]. All other strains were routinely grown at 37 °C on LB agar and in LB broth (cat# 244520 and 244620, Becton & Dickinson Co., Franklin Lakes, NJ, USA) unless otherwise specified.

4.2. Deletion Plasmid Construction

PAO1 strains carrying full deletions of *mexAB*, *mexEF*, or *mexR* genes listed in Table S1 were generated with a suicide plasmid as described previously [50]. For the Δ *mexAB* and Δ *mexR* strains, two PCR fragments were generated from chromosomal DNA for each construct using the following primer pairs up- and down-stream of each target for mutation; *mexAB* genes: *mexAB*-KO-UP-F and *mexAB*-KO-UP-R for the upstream *mexAB* fragment and *mexAB*-KO-DN-F and *mexAB*-KO-DN-R for the downstream *mexAB* fragment; and *mexR*: *mexR*-KO-UP-F and *mexR*-KO-UP-R for the upstream *mexR* fragment and *mexR*-KO-DN-F and *mexR*-KO-DN-R for the downstream *mexR* fragment. The suicide plasmid pEX18Gm [51] was prepared for assembly by restriction digest or PCR amplification with primers pEX18Gm-F and pEX18Gm-R (Supplementary Material Table S1). The two fragments for each construct were then assembled into the prepared vector pEX18Gm [51] using NEBuilder HiFi DNA Assembly Cloning Kit (cat# E5520, New England BioLabs, Ipswich, MA, USA) for the Δ *mexAB* mutant and the NEB Gibson Assembly Master Mix (cat# E2611L, New England BioLabs, Ipswich, MA, USA) for the Δ *mexR* mutant. Suicide plasmids were transformed into *E. coli* DH5 α [52] competent cells (NEB cat# C2987H, New England BioLabs, Ipswich, MA, USA) according to manufacturer's protocol, selected on LB agar with 10 μ g/mL gentamicin (Gm). Plasmids were isolated using the NEB Monarch Plasmid Purification MiniPrep Kit (cat# T1010L, New England BioLabs, Ipswich, MA, USA) and verified by Sanger sequencing. For the Δ *mexEF* mutant construct, two sets of primers (oRP_21, oRP_22 and oRP_23, oRP_24) were designed to amplify 527 and 495 bp regions upstream and downstream, respectively, of the *mexEF* genes. These PCR fragments were assembled by splicing by overlap extension PCR and the deletion allele, containing attachment sites (*attB1*- and *attB2*-) for Gateway recombination, was integrated into the pDONRPEX18Gm vector via the BP Clonase reaction, as previously described [50]. The reaction mixture was transformed into *E. coli* DH5 α by electroporation, and clones harboring the plasmid with the Δ *mexEF* allele were selected on LB agar with 10 μ g/mL Gm and identified by colony PCR using M13 universal primers. This yielded plasmid pRP12 (pDONRPEX18Gm:: Δ *mexEF*), which was sequence verified using M13 primers.

4.3. Transformation of *P. aeruginosa* Deletion Mutants

PAO1 deletion mutants were generated from WT *P. aeruginosa* PAO1 through two-step allelic exchange through either electroporation or mating, as described previously [50]. For electroporation of pEX18Gm:: Δ *mexAB*, 1.5 mL of PAO1 or PAO1-AzEvB8 grown overnight in LB were centrifuged at $14,000\times g$ for 3 min and washed twice with 300 mM sterile sucrose. Cells were then centrifuged at $14,000\times g$ for 3 min and resuspended in 100 μ L of 300 mM sterile sucrose. One microgram of pEX18Gm:: Δ *mexAB* was then added to each cell suspension, and the bacterial suspensions were transformed by electroporation at 2.5 kV and incubated on LB with 30 μ g/mL Gm at 37 °C overnight. For counter selection, isolated clones were streaked on low-salt LB containing 15% sucrose as published [50] and incubated at room temperature for 48 h. Gene deletions were confirmed by PCR using primers *mexAB*-KO-Chk-F and *mexAB*-KO-Chk-R (Table S1) and Sanger sequencing. For the Δ *mexR* strain, pEX18Gm:: Δ *mexR* was transformed into chemically competent *E. coli* SM10(λ _{pir}) [53] which were prepared using transformation and storage solution (TSS, LB broth with 10% (w/v) polyethylene glycol, 5% (v/v) dimethyl sulfoxide, and 0.5% (w/v) MgSO₄·7H₂O), as described previously [54] and selection on LB agar with 20 μ g/mL Gm. *E. coli* SM10(λ _{pir}) pEX18Gm:: Δ *mexR* was mixed with PAO1, spotted onto an LB plate, and incubated overnight at 30 °C. Matings were collected and plated on VBMM agar with 60 μ g/mL Gm to select for *P. aeruginosa* merodiploids and incubated overnight at 37 °C, as described [50]. Merodiploid colonies were streaked onto LB agar with 15% sucrose and incubated at 25 °C for 4 days. PAO1 Δ *mexR* strains were confirmed by PCR amplification using primers *mexR*-KO-UP-F and *mexR*-KO-DN-R (Table S1). To generate the PAO1 Δ *mexEF* strain, pDONRPEX18Gm:: Δ *mexEF* was transformed into the donor *E. coli* S.17.1 (λ _{pir}) strain. Biparental mating was used to introduce the suicide plasmid into

the *P. aeruginosa* PAO1 recipient. Merodiploids resistant to sucrose but sensitive to Gm were isolated by counter-selection on no-salt-LB agar with 15% *w/v* sucrose after two days of incubation at 30 °C. Colony PCR was performed to identify $\Delta mexEF$ mutants and PCR products generated from the cloned mutant allele were sent for sequencing with oRP_27 and oRP_28 primers. Using this protocol, a 4397 bp fragment from the 4434 bp *mexEF* sequence was removed resulting in a frameshift mutation in the *mexEF-oprN* multidrug efflux operon, yielding strain RP05 (PAO1 $\Delta mexEF$) (Table S1).

4.4. PAO1 Transformation with *rhIA* Reporter Plasmid

To quantify the expression of genes involved in rhamnolipid production, strains PAO1, PAO1-AvEvB8, PAO1 $\Delta mexR$, PAO1 $\Delta mexEF$, and PAO1 $\Delta mexAB$ were transformed with pYL122, a plasmid containing *rhIA-gfp* promoter fusion in a mini-CTX-*lacZ* backbone [55]. Following transformation, strains were maintained on LB plates with 100 µg/mL tetracycline. Clones were then tested using PCR with the primers pYL122-Chk-F and pYL122-Chk-R (Table S1).

4.5. DNA Extraction, Purification, and PCR

Plasmid DNA was prepared using Monarch Plasmid Miniprep Kit (cat# T1010, New England BioLabs, Ipswich, MA, USA). Genomic DNA was prepared using DNeasy Blood & Tissue Kit (cat# 69504, Qiagen, Hilden, Germany). When necessary, cDNA was purified using Monarch PCR & DNA Cleanup Kit (cat# T1030, New England BioLabs, Ipswich, MA, USA). PCR was performed using either KAPA HIFI 2X ready mix (cat# KK2602, KAPA Biosystems, Wilmington, MA, USA).

4.6. Swarming Assay

Swarming plates were created using 2.5% LB and 0.5% agar. For the assay, all strains were grown overnight for 16–20 h in LB broth without antibiotics, including Tn mutants. For each strain, 2 µL of the overnight broth was then placed at the center of a swarming plate and left to incubate at 37 °C for 24 h. The maximum swarming diameter was then measured and recorded for each strain.

4.7. Gradient Diffusion Antibiotic Susceptibility Testing

Aztreonam, ciprofloxacin, and chloramphenicol Etest strips were purchased from bioMérieux (cat# 501758, 412310, 412308, Durham, NC, USA) and antimicrobial susceptibility testing was performed with the following modifications to the manufacturer's instructions. For aztreonam, a sterile swab was soaked in an overnight culture for each strain after growth for 18 h in LB broth and excess fluid was removed by pressing it against the inside wall of the test tube. For ciprofloxacin and chloramphenicol, colonies were picked directly from LB agar plates and diluted in sterile PBS to OD₆₀₀ 0.15 ($\sim 1.5 \times 10^8$ CFU/mL). Mueller Hinton agar plates were fully streaked 4 times with the swabs. After allowing the plates to dry, an Etest gradient strip was placed in the middle of the plates. Plates were incubated at 37 °C for 16–20 h.

4.8. *rhIA* GFP Reporter Assay

WT PAO1, PAO1 *attB::rhIA-gfp*, PAO1-AzEvB8, PAO1-AzEvB8 *attB::rhIA-gfp*, $\Delta mexR$, $\Delta mexR$ *attB::rhIA-gfp*, $\Delta mexEF$, $\Delta mexEF$ *attB::rhIA-gfp*, $\Delta mexAB$, and $\Delta mexAB$ *attB::rhIA-gfp* strains were grown overnight for 16–20 h in 2 mL LB. The overnight cultures were then diluted to OD₆₀₀ ~ 0.005 ($\sim 5 \times 10^6$ CFU/mL). Two hundred microliters of the working dilutions were added in triplicate to a sterile black (clear bottom) 96-well plate. To prevent evaporation, 50 µL of mineral oil was added to each well. The plate was incubated for 24 h at 37 °C, shaking at 250 rpm, and absorbance at 600 nm and fluorescence with excitation at 488 nm and emission at 510 nm were read every hour for 24 h. For each strain, fluorescence was first normalized to the absorbance value. The background of each nontransformed strain was then subtracted from its pYL122-carrying counterpart. Gene expression was

calculated as area under the curve using Prism GraphPad. For the efflux pump inhibitor assay, the *rhlA* reporter assay was performed as described above with the exception that the efflux pump inhibitor PA β N (Phe-Arg β -naphthylamide dihydrochloride, Sigma-Aldrich, Burlington, MA, USA, cat# P4157-25MG) was added to cultures to reach final concentrations of 0 μ g/mL, 5 μ g/mL, 10 μ g/mL, and 25 μ g/mL.

4.9. Murine Lung Infection

Experiments were approved by the Institutional Animal Care and Use Committee at Cedars-Sinai Medical Center under protocol IACUC008115. Strains were grown to mid-exponential phase, washed with sterile PBS, and diluted to 1×10^8 CFU/mL in sterile PBS. Female C57BL/6 (Jackson Laboratories, Bar Harbor, ME, USA) 12-week-old mice (10 mice/group) were anesthetized using isoflurane. A 24-gauge angiocatheter was used to intubate the mice. Acute lung infections were performed by single intratracheal instillations of 5×10^6 CFUs in 50 μ L sterile PBS. During inoculation the mice were placed on a surgical board in the supine position. The front paws of each mouse were stretched outwards. A rubber band was placed around the two front incisors of the mouse to help keep their mouths open during the intubation procedure. After inoculation mice were kept in a clean cage under infrared lamp until full recovery. Mice were evaluated thrice per day to assess morbidity, and moribund mice were sacrificed with inhaled CO₂. Surviving mice were euthanized 96 h post-infection. Survival curves were analyzed with log-rank tests as described below.

4.10. Genome Sequencing and Analysis

To verify mutations in engineered *P. aeruginosa* strains, DNA was isolated from strains PAO1, PAO1 Δ *mexAB*, PAO1-AzEvB8, PAO1-AzEvB8 Δ *mexAB*, and PAO1 Δ *mexEF* and subjected to whole genome sequencing. DNA isolation was performed using a DNeasy Blood and Tissue Kit (Qiagen, Hilden, Germany). DNA was submitted to the Microbial Genome Sequencing Center at the University of Pittsburgh where libraries were prepared and sequenced using an Illumina NextSeq platform. Sequencing reads were analyzed using Breseq [56], comparing reads for each strain to the *P. aeruginosa* PAO1 parent reference genome. Figure showing deletion in the *P. aeruginosa* PAO1-AzEvB8 strain was created using CLC Genomics Workbench Software.

4.11. Statistics

Statistical analyses were performed using Prism GraphPad Software v9 and SAS. For swarming and *rhlA* reporter assays, one-way ANOVA tests were performed followed by Tukey's multiple comparison test. For survival analyses, survival times were tested across strata with a log-rank test, with Bonferroni-adjusted *p*-values where >2 strata were compared.

5. Conclusions

Altogether, this work sheds important light on how antibiotic-resistance mutations can affect efflux pumps and subsequent *P. aeruginosa* virulence. Long-term, we believe that new strategies for treating efflux pump overexpression or deletion mutants should be pursued. It will be particularly important to study the effects of efflux pump mutations in the context of biofilms and aggregates, both in vitro and in vivo, because this is the predominant bacterial mode of growth during CF infections. Additionally, we plan to explore how *mexR* mutations lead to increased virulence, since this mechanism still remains mysterious.

Supplementary Materials: The following are available online at <https://www.mdpi.com/article/10.3390/antibiotics10101164/s1>, Table S1: Strains and primers used in this study.

Author Contributions: Conceptualization, M.V. and P.J.; methodology, M.V. and P.J.; formal analysis, M.V., S.P.L., C.B. and P.J.; investigation, M.V., S.P.L., C.B., R.P. and P.J.; resources, R.P. and P.J.; data

curation, M.V., S.P.L., C.B. and P.J.; writing—original draft preparation, M.V., S.P.L., R.P. and P.J.; writing—review and editing, M.V., S.P.L., C.B., R.P. and P.J.; supervision, M.V. and P.J.; project administration, M.V. and P.J.; funding acquisition, P.J. All authors have read and agreed to the published version of the manuscript.

Funding: This research was funded by grant numbers JORTH17F5 and JORTH19P0 from the Cystic Fibrosis Foundation and grant numbers K22AI127473 and R01AI14642 from the NIH/National Institute of Allergy and Infectious Diseases, as well as a sub-award from grant number UL1TR001881 from the NIH/National Center for Advancing Translational Science (NCATS) UCLA CTSI.

Institutional Review Board Statement: The study was conducted according to the guidelines of the Declaration of Helsinki and approved by the Institutional Animal Care and Use Committee of Cedars-Sinai Medical Center (protocol code IACUC008115 approved on May 23, 2018).

Informed Consent Statement: Not applicable.

Data Availability Statement: Genome sequencing data are available through the National Center for Biotechnology Information (NCBI) Sequence Read Archive through BioProject accession number: PRJNA766087, <http://www.ncbi.nlm.nih.gov/bioproject/766087>.

Acknowledgments: We would like to thank members of the Jorth Lab, Joe Harrison, and Holly Huse for helpful discussions and feedback on this manuscript. We are grateful to Pradeep K. Singh, Colin Manoil, and Joe J. Harrison for the generous gifts of strains for this study.

Conflicts of Interest: The authors declare no conflict of interest.

References

1. Silby, M.W.; Winstanley, C.; Godfrey, S.A.; Levy, S.B.; Jackson, R.W. *Pseudomonas* genomes: Diverse and adaptable. *FEMS Microbiol. Rev.* **2011**, *35*, 652–680. [\[CrossRef\]](#)
2. Moradali, M.F.; Ghods, S.; Rehm, B.H. *Pseudomonas aeruginosa* Lifestyle: A Paradigm for Adaptation, Survival, and Persistence. *Front. Cell Infect. Microbiol.* **2017**, *7*, 39. [\[CrossRef\]](#)
3. Morrison, A.J., Jr.; Wenzel, R.P. Epidemiology of infections due to *Pseudomonas aeruginosa*. *Rev. Infect. Dis.* **1984**, *6* (Suppl. S3), S627–S642. [\[CrossRef\]](#) [\[PubMed\]](#)
4. Parkins, M.D.; Somayaji, R.; Waters, V.J. Epidemiology, Biology, and Impact of Clonal *Pseudomonas aeruginosa* Infections in Cystic Fibrosis. *Clin. Microbiol. Rev.* **2018**, *31*, e00019–18. [\[CrossRef\]](#) [\[PubMed\]](#)
5. Jain, M.; Ramirez, D.; Seshadri, R.; Cullina, J.F.; Powers, C.A.; Schulert, G.S.; Bar-Meir, M.; Sullivan, C.L.; McColley, S.A.; Hauser, A.R. Type III secretion phenotypes of *Pseudomonas aeruginosa* strains change during infection of individuals with cystic fibrosis. *J. Clin. Microbiol.* **2004**, *42*, 5229–5237. [\[CrossRef\]](#)
6. Smith, E.E.; Buckley, D.G.; Wu, Z.; Saenphimmachak, C.; Hoffman, L.R.; D’Argenio, D.A.; Miller, S.I.; Ramsey, B.W.; Speert, D.P.; Moskowitz, S.M.; et al. Genetic adaptation by *Pseudomonas aeruginosa* to the airways of cystic fibrosis patients. *Proc. Natl. Acad. Sci. USA* **2006**, *103*, 8487–8492. [\[CrossRef\]](#) [\[PubMed\]](#)
7. Huse, H.K.; Kwon, T.; Zlosnik, J.E.; Speert, D.P.; Marcotte, E.M.; Whiteley, M. Parallel evolution in *Pseudomonas aeruginosa* over 39,000 generations in vivo. *mBio* **2010**, *1*, e00199–10. [\[CrossRef\]](#)
8. Jorth, P.; Staudinger, B.J.; Wu, X.; Hisert, K.B.; Hayden, H.; Garudathri, J.; Harding, C.L.; Radey, M.C.; Rezayat, A.; Bautista, G.; et al. Regional Isolation Drives Bacterial Diversification within Cystic Fibrosis Lungs. *Cell Host Microbe* **2015**, *18*, 307–319. [\[CrossRef\]](#)
9. Winstanley, C.; O’Brien, S.; Brockhurst, M.A. *Pseudomonas aeruginosa* Evolutionary Adaptation and Diversification in Cystic Fibrosis Chronic Lung Infections. *Trends Microbiol.* **2016**, *24*, 327–337. [\[CrossRef\]](#)
10. Darch, S.E.; McNally, A.; Harrison, F.; Corander, J.; Barr, H.L.; Paszkiewicz, K.; Holden, S.; Fogarty, A.; Crusz, S.A.; Diggle, S.P. Recombination is a key driver of genomic and phenotypic diversity in a *Pseudomonas aeruginosa* population during cystic fibrosis infection. *Sci. Rep.* **2015**, *5*, 7649. [\[CrossRef\]](#)
11. O’Brien, S.; Williams, D.; Fothergill, J.L.; Paterson, S.; Winstanley, C.; Brockhurst, M.A. High virulence sub-populations in *Pseudomonas aeruginosa* long-term cystic fibrosis airway infections. *BMC Microbiol.* **2017**, *17*, 30. [\[CrossRef\]](#)
12. Faure, E.; Kwong, K.; Nguyen, D. *Pseudomonas aeruginosa* in Chronic Lung Infections: How to Adapt within the Host? *Front. Immunol.* **2018**, *9*, 2416. [\[CrossRef\]](#)
13. Jensen, P.O.; Bjarnsholt, T.; Phipps, R.; Rasmussen, T.B.; Calum, H.; Christoffersen, L.; Moser, C.; Williams, P.; Pressler, T.; Givskov, M.; et al. Rapid necrotic killing of polymorphonuclear leukocytes is caused by quorum-sensing-controlled production of rhamnolipid by *Pseudomonas aeruginosa*. *Microbiology* **2007**, *153*, 1329–1338. [\[CrossRef\]](#)
14. Zulianello, L.; Canard, C.; Kohler, T.; Caille, D.; Lacroix, J.S.; Meda, P. Rhamnolipids are virulence factors that promote early infiltration of primary human airway epithelia by *Pseudomonas aeruginosa*. *Infect. Immun.* **2006**, *74*, 3134–3147. [\[CrossRef\]](#)
15. Lavoie, E.G.; Wangdi, T.; Kazmierczak, B.I. Innate immune responses to *Pseudomonas aeruginosa* infection. *Microbes Infect.* **2011**, *13*, 1133–1145. [\[CrossRef\]](#)

16. Mogayzel, P.J., Jr.; Naureckas, E.T.; Robinson, K.A.; Brady, C.; Guill, M.; Lahiri, T.; Lubsch, L.; Matsui, J.; Oermann, C.M.; Ratjen, F.; et al. Cystic Fibrosis Foundation pulmonary guideline. pharmacologic approaches to prevention and eradication of initial *Pseudomonas aeruginosa* infection. *Ann. Am. Thorac Soc.* **2014**, *11*, 1640–1650. [\[CrossRef\]](#)
17. Sobel, M.L.; Hocquet, D.; Cao, L.; Plesiat, P.; Poole, K. Mutations in PA3574 (nalD) lead to increased MexAB-OprM expression and multidrug resistance in laboratory and clinical isolates of *Pseudomonas aeruginosa*. *Antimicrob. Agents Chemother.* **2005**, *49*, 1782–1786. [\[CrossRef\]](#) [\[PubMed\]](#)
18. Poole, K.; Tetro, K.; Zhao, Q.; Neshat, S.; Heinrichs, D.E.; Bianco, N. Expression of the multidrug resistance operon mexA-mexB-oprM in *Pseudomonas aeruginosa*: mexR encodes a regulator of operon expression. *Antimicrob. Agents Chemother.* **1996**, *40*, 2021–2028. [\[CrossRef\]](#) [\[PubMed\]](#)
19. Saito, K.; Yoneyama, H.; Nakae, T. nalB-type mutations causing the overexpression of the MexAB-OprM efflux pump are located in the mexR gene of the *Pseudomonas aeruginosa* chromosome. *FEMS Microbiol. Lett.* **1999**, *179*, 67–72. [\[CrossRef\]](#) [\[PubMed\]](#)
20. Jorth, P.; McLean, K.; Ratjen, A.; Secor, P.R.; Bautista, G.E.; Ravishankar, S.; Rezayat, A.; Garudathri, J.; Harrison, J.J.; Harwood, R.A.; et al. Evolved Aztreonam Resistance Is Multifactorial and Can Produce Hypervirulence in *Pseudomonas aeruginosa*. *mBio* **2017**, *8*, e00517-17. [\[CrossRef\]](#)
21. Suresh, M.; Nithya, N.; Jayasree, P.R.; Vimal, K.P.; Manish Kumar, P.R. Mutational analyses of regulatory genes, mexR, nalC, nalD and mexZ of mexAB-oprM and mexXY operons, in efflux pump hyperexpressing multidrug-resistant clinical isolates of *Pseudomonas aeruginosa*. *World J. Microbiol. Biotechnol.* **2018**, *34*, 83. [\[CrossRef\]](#)
22. Horna, G.; Lopez, M.; Guerra, H.; Saenz, Y.; Ruiz, J. Interplay between MexAB-OprM and MexEF-OprN in clinical isolates of *Pseudomonas aeruginosa*. *Sci. Rep.* **2018**, *8*, 16463. [\[CrossRef\]](#)
23. Llanes, C.; Hocquet, D.; Vogne, C.; Benali-Baitich, D.; Neuwirth, C.; Plesiat, P. Clinical strains of *Pseudomonas aeruginosa* overproducing MexAB-OprM and MexXY efflux pumps simultaneously. *Antimicrob. Agents Chemother.* **2004**, *48*, 1797–1802. [\[CrossRef\]](#)
24. McLean, K.; Lee, D.; Holmes, E.A.; Penewit, K.; Waalkes, A.; Ren, M.; Lee, S.A.; Gasper, J.; Manoil, C.; Salipante, S.J. Genomic Analysis Identifies Novel *Pseudomonas aeruginosa* Resistance Genes under Selection during Inhaled Aztreonam Therapy In Vivo. *Antimicrob. Agents Chemother.* **2019**, *63*, e00866-19. [\[CrossRef\]](#)
25. Oshri, R.D.; Zrihen, K.S.; Shner, I.; Omer Bendori, S.; Eldar, A. Selection for increased quorum-sensing cooperation in *Pseudomonas aeruginosa* through the shut-down of a drug resistance pump. *ISME J.* **2018**, *12*, 2458–2469. [\[CrossRef\]](#)
26. Kohler, T.; van Delden, C.; Curty, L.K.; Hamzehpour, M.M.; Pechere, J.C. Overexpression of the MexEF-OprN multidrug efflux system affects cell-to-cell signaling in *Pseudomonas aeruginosa*. *J. Bacteriol.* **2001**, *183*, 5213–5222. [\[CrossRef\]](#)
27. Lomovskaya, O.; Warren, M.S.; Lee, A.; Galazzo, J.; Fronko, R.; Lee, M.; Blais, J.; Cho, D.; Chamberland, S.; Renau, T.; et al. Identification and characterization of inhibitors of multidrug resistance efflux pumps in *Pseudomonas aeruginosa*: Novel agents for combination therapy. *Antimicrob. Agents Chemother.* **2001**, *45*, 105–116. [\[CrossRef\]](#) [\[PubMed\]](#)
28. Cosson, P.; Zulianello, L.; Join-Lambert, O.; Faurisson, F.; Gebbie, L.; Benghezal, M.; van Delden, C.; Curty, L.K.; Kohler, T. *Pseudomonas aeruginosa* virulence analyzed in a Dictyostelium discoideum host system. *J. Bacteriol.* **2002**, *184*, 3027–3033. [\[CrossRef\]](#) [\[PubMed\]](#)
29. Hirakata, Y.; Kondo, A.; Hoshino, K.; Yano, H.; Arai, K.; Hirotsu, A.; Kunishima, H.; Yamamoto, N.; Hatta, M.; Kitagawa, M.; et al. Efflux pump inhibitors reduce the invasiveness of *Pseudomonas aeruginosa*. *Int. J. Antimicrob. Agents* **2009**, *34*, 343–346. [\[CrossRef\]](#) [\[PubMed\]](#)
30. Rampioni, G.; Pillai, C.R.; Longo, F.; Bondi, R.; Baldelli, V.; Messina, M.; Imperi, F.; Visca, P.; Leoni, L. Effect of efflux pump inhibition on *Pseudomonas aeruginosa* transcriptome and virulence. *Sci. Rep.* **2017**, *7*, 11392. [\[CrossRef\]](#) [\[PubMed\]](#)
31. Miyata, S.; Casey, M.; Frank, D.W.; Ausubel, F.M.; Drenkard, E. Use of the Galleria mellonella caterpillar as a model host to study the role of the type III secretion system in *Pseudomonas aeruginosa* pathogenesis. *Infect. Immun.* **2003**, *71*, 2404–2413. [\[CrossRef\]](#)
32. Kropinski, A.M.; Chadwick, J.S. The pathogenicity of rough strains of *Pseudomonas aeruginosa* for Galleria mellonella. *Can. J. Microbiol.* **1975**, *21*, 2084–2088. [\[CrossRef\]](#) [\[PubMed\]](#)
33. Marvig, R.L.; Sommer, L.M.; Molin, S.; Johansen, H.K. Convergent evolution and adaptation of *Pseudomonas aeruginosa* within patients with cystic fibrosis. *Nat. Genet.* **2015**, *47*, 57–64. [\[CrossRef\]](#) [\[PubMed\]](#)
34. Fukuda, H.; Hosaka, M.; Hirai, K.; Iyobe, S. New norfloxacin resistance gene in *Pseudomonas aeruginosa* PAO. *Antimicrob. Agents Chemother.* **1990**, *34*, 1757–1761. [\[CrossRef\]](#) [\[PubMed\]](#)
35. Kohler, T.; Michea-Hamzehpour, M.; Henze, U.; Gotoh, N.; Curty, L.K.; Pechere, J.C. Characterization of MexE-MexF-OprN, a positively regulated multidrug efflux system of *Pseudomonas aeruginosa*. *Mol. Microbiol.* **1997**, *23*, 345–354. [\[CrossRef\]](#) [\[PubMed\]](#)
36. Quale, J.; Bratu, S.; Gupta, J.; Landman, D. Interplay of efflux system, ampC, and oprD expression in carbapenem resistance of *Pseudomonas aeruginosa* clinical isolates. *Antimicrob. Agents Chemother.* **2006**, *50*, 1633–1641. [\[CrossRef\]](#)
37. Tomas, M.; Doumith, M.; Warner, M.; Turton, J.F.; Beceiro, A.; Bou, G.; Livermore, D.M.; Woodford, N. Efflux pumps, OprD porin, AmpC beta-lactamase, and multiresistance in *Pseudomonas aeruginosa* isolates from cystic fibrosis patients. *Antimicrob. Agents Chemother.* **2010**, *54*, 2219–2224. [\[CrossRef\]](#)
38. Keating, C.L.; Zuckerman, J.B.; Singh, P.K.; McKevitt, M.; Gurtovaya, O.; Bresnik, M.; Marshall, B.C.; Saiman, L. *Pseudomonas aeruginosa* Susceptibility Patterns and Associated Clinical Outcomes in People with Cystic Fibrosis following Approval of Aztreonam Lysine for Inhalation. *Antimicrob. Agents Chemother.* **2021**, *65*, e02327-20. [\[CrossRef\]](#)

39. Yoshida, K.; Nakayama, K.; Ohtsuka, M.; Kuru, N.; Yokomizo, Y.; Sakamoto, A.; Takemura, M.; Hoshino, K.; Kanda, H.; Nitani, H.; et al. MexAB-OprM specific efflux pump inhibitors in *Pseudomonas aeruginosa*. Part 7: Highly soluble and in vivo active quaternary ammonium analogue D13-9001, a potential preclinical candidate. *Bioorg. Med. Chem.* **2007**, *15*, 7087–7097. [[CrossRef](#)]
40. Roux, D.; Danilchanka, O.; Guillard, T.; Cattoir, V.; Aschard, H.; Fu, Y.; Angoulvant, F.; Messika, J.; Ricard, J.D.; Mekalanos, J.J.; et al. Fitness cost of antibiotic susceptibility during bacterial infection. *Sci. Transl. Med.* **2015**, *7*, 297ra114. [[CrossRef](#)]
41. Cowley, E.S.; Kopf, S.H.; LaRiviere, A.; Ziebis, W.; Newman, D.K. Pediatric Cystic Fibrosis Sputum Can Be Chemically Dynamic, Anoxic, and Extremely Reduced Due to Hydrogen Sulfide Formation. *mBio* **2015**, *6*, e00767-15. [[CrossRef](#)] [[PubMed](#)]
42. Palmer, K.L.; Brown, S.A.; Whiteley, M. Membrane-bound nitrate reductase is required for anaerobic growth in cystic fibrosis sputum. *J. Bacteriol.* **2007**, *189*, 4449–4455. [[CrossRef](#)] [[PubMed](#)]
43. Palmer, K.L.; Aye, L.M.; Whiteley, M. Nutritional cues control *Pseudomonas aeruginosa* multicellular behavior in cystic fibrosis sputum. *J. Bacteriol.* **2007**, *189*, 8079–8087. [[CrossRef](#)] [[PubMed](#)]
44. Turner, K.H.; Wessel, A.K.; Palmer, G.C.; Murray, J.L.; Whiteley, M. Essential genome of *Pseudomonas aeruginosa* in cystic fibrosis sputum. *Proc. Natl. Acad. Sci. USA* **2015**, *112*, 4110–4115. [[CrossRef](#)] [[PubMed](#)]
45. Rogers, C.S.; Stoltz, D.A.; Meyerholz, D.K.; Ostedgaard, L.S.; Rokhlina, T.; Taft, P.J.; Rogan, M.P.; Pezzulo, A.A.; Karp, P.H.; Itani, O.A.; et al. Disruption of the CFTR gene produces a model of cystic fibrosis in newborn pigs. *Science* **2008**, *321*, 1837–1841. [[CrossRef](#)] [[PubMed](#)]
46. Starke, J.R.; Edwards, M.S.; Langston, C.; Baker, C.J. A mouse model of chronic pulmonary infection with *Pseudomonas aeruginosa* and *Pseudomonas cepacia*. *Pediatr. Res.* **1987**, *22*, 698–702. [[CrossRef](#)]
47. Van Heeckeren, A.M.; Schluchter, M.D. Murine models of chronic *Pseudomonas aeruginosa* lung infection. *Lab. Anim.* **2002**, *36*, 291–312. [[CrossRef](#)]
48. Van Heeckeren, A.M.; Schluchter, M.D.; Drumm, M.L.; Davis, P.B. Role of Cftr genotype in the response to chronic *Pseudomonas aeruginosa* lung infection in mice. *Am. J. Physiol. Lung Cell. Mol. Physiol.* **2004**, *287*, L944–L952. [[CrossRef](#)]
49. Held, K.; Ramage, E.; Jacobs, M.; Gallagher, L.; Manoil, C. Sequence-verified two-allele transposon mutant library for *Pseudomonas aeruginosa* PAO1. *J. Bacteriol.* **2012**, *194*, 6387–6389. [[CrossRef](#)]
50. Hmelo, L.R.; Borlee, B.R.; Almblad, H.; Love, M.E.; Randall, T.E.; Tseng, B.S.; Lin, C.; Irie, Y.; Storek, K.M.; Yang, J.J.; et al. Precision-engineering the *Pseudomonas aeruginosa* genome with two-step allelic exchange. *Nat. Protoc.* **2015**, *10*, 1820–1841. [[CrossRef](#)]
51. Hoang, T.T.; Karkhoff-Schweizer, R.R.; Kutchma, A.J.; Schweizer, H.P. A broad-host-range Flp-FRT recombination system for site-specific excision of chromosomally-located DNA sequences: Application for isolation of unmarked *Pseudomonas aeruginosa* mutants. *Gene* **1998**, *212*, 77–86. [[CrossRef](#)]
52. Taylor, R.G.; Walker, D.C.; McInnes, R.R.E. coli host strains significantly affect the quality of small scale plasmid DNA preparations used for sequencing. *Nucleic Acids Res.* **1993**, *21*, 1677–1678. [[CrossRef](#)] [[PubMed](#)]
53. Simon, R.; Priefer, U.; Pühler, A. A Broad Host Range Mobilization System for In Vivo Genetic Engineering: Transposon Mutagenesis in Gram Negative Bacteria. *Nat. Biotechnol.* **1983**, *1*, 784–791. [[CrossRef](#)]
54. Chung, C.T.; Niemela, S.L.; Miller, R.H. One-step preparation of competent *Escherichia coli*: Transformation and storage of bacterial cells in the same solution. *Proc. Natl. Acad. Sci. USA* **1989**, *86*, 2172–2175. [[CrossRef](#)] [[PubMed](#)]
55. Lequette, Y.; Greenberg, E.P. Timing and localization of rhamnolipid synthesis gene expression in *Pseudomonas aeruginosa* biofilms. *J. Bacteriol.* **2005**, *187*, 37–44. [[CrossRef](#)]
56. Deatherage, D.E.; Barrick, J.E. Identification of mutations in laboratory-evolved microbes from next-generation sequencing data using breseq. *Methods Mol. Biol.* **2014**, *1151*, 165–188. [[CrossRef](#)] [[PubMed](#)]